International Journal of Concrete Structures and Materials
Vol.8, No.1, pp.15–26, March 2014
DOI 10.1007/s40069-013-0066-8
ISSN 1976-0485 / eISSN 2234-1315

Use of Bentonite and Organobentonite as Alternatives of Partial Substitution of Cement in Concrete Manufacturing

D. J. Lima-Guerra*, I. Mello, R. Resende, and R. Silva

(Received April 8, 2013, Accepted December 29, 2013)

Abstract: In order to study the capacities of a new occurrence of Brazilian clay samples as partial replacements of cement, a bentonite sample was selected for utilization in the natural and modified forms for present study. The natural bentonite (BBT) was modified by anchorament of 3-aminopropyltrietoxisilane (BBT_{APS}) and 3,2-aminoethylaminopropyltrimetoxisilane (BBT_{AEAPS}) in the surface of component minerals of bentonite sample. The original and organo-bentonite samples were characterized by elemental analysis, scanning electron microscopic and textural analyses. The values of micropore area were varying from 7.2 $m^2\ g^{-1}$ for the BBT to 12.3 $m^2\ g^{-1}$ for the BBT_{AEAPS}. The bentonite samples were characterized by the main variable proportion of bentonite in the natural and intercalated forms (2, 5, 10, 15, 20, 25, 30, and 35 % by weight of cement) in the replacement mode whiles the amount of cementations material. The workability, density of fresh concrete, and absorption of water decreased as the substitution of ordinary Portland cement by perceptual of natural and modified bentonite increased. The results reveal that workability decreased with decrease of the amount of natural bentonite in the concrete, same behavior is observed for bentonite functionalized, varying from 49 to 28 mm. The energetic influence of the interaction of calcium nitrate in the structure of blends was determined through the calorimetric titration procedure.

Keywords: bentonite, intercalation, workability, fresh concrete density, thermodynamic.

1. Introduction

Clay minerals and organoclays are widely used as adsorbents due to their textural and physical–chemical characteristics, such as: high specific area, pore size diameter, cation exchange capacity (CEC), and hydrophilic particles that can be formed their reactive surfaces. As a petrographical definition, bentonite is a geological material composed from volcanic ashes altered in shallow sea and lagoons areas and generally formed by phyllosilicates, such as smectite types, which is a 2:1 mineral, consists of two tetrahedral sheets (silicon/oxygen) separated by an octahedral sheet (aluminum/oxygen/hydroxyl) (Meunier 2005; Bulut et al. 2009). The ions with positive charges on the clay surface can be adsorbed onto the structure bentonite owing to the interaction between the negative and positive charge, in addition, bentonite clay is used in chemical and ceramic industries for fabrication of several ceramic products owing to the rheological properties, this phyllosilicate types are recommended to the fabrication of beds for utilization as desiccators or as dehydrator of various gases. The industrial and environmental applications of bentonite have showed an upsurge of interest in recent years; various abundant minerals and clay minerals have been utilized in manufacturing process of cement, and they included: kaolinite, goethite, dolomite, cristobalite, and palykorskite (Bojumueller et al. 2001; Taylor-Lange et al. 2012). The utilization of bentonite/cement slurry trench cut-off walls, peculiarly in the highly attackable environments, raises concerns over durability, The durability and physical–chemical interactions of the bentonite clay type and cement, blend used as cut-off walls are important factors in determining their potential service life and how long they will function properly in the soils (Plee et al. 1990; Garvin and Hayles 1999; Shannag 2000). There is limited data available as partial replacements of cement in concrete using Brazilian bentonite samples.

The chemistry of intercalation is a research area that has been widely investigated and plays a very important part in applications in many academic and technological fields, such as those related to ion-exchange reactions and supports for catalytic methods (Meunier 2005; Bulut et al. 2009; Mirza et al. 2009; Ahmad et al. 2011). The insertion process of organic neutral polar molecules into the nanospace void of sheets of layered insoluble nanocompounds leads to well-organized inorganic/organic structural layer materials with high crystallinity and porosity (Guerra et al. 2006, 2009, 2011; Diaz et al. 2007; Lazarin and Airoldi 2009). Important advances in the organofunctionalization processes field have been obtained by observing if any property of the lamellar nanocompound charges, by comparing these with those

University Federal of Mato Grosso, DRM-UFMT, Cuiaba, Mato Grosso 78060 900, Brazil.
*Corresponding Author; E-mail: denis@cpd.ufmt.br, dlguerra@pq.cnpq.br

related to the host, as well as to the inserted guest molecules at the end of the process (Zhang et al. 2000; Ogawa et al. 2003; Chaudhari and Kumar 2005; Dey and Airoldi 2008). various investigations on intercalating of a variety of amine, such as secondary, tertiary, cyclic or arylic amines into lamellar compounds have been reported (Goubitz et al. 2001; Ogawa et al. 2003). These species are of interest not only in order to further clarity the chemistry of layered metal but also because the process leads to the preparation and characterization of a new intercalated phase of hybrid material (Sharma et al. 2009).

The purpose of this investigation therefore is to obtain an understanding of application of new occurrence of Amazon bentonite by studying the influence of intercalation processes in the utilization of natural (BBT) and modified bentonite samples (BBT_{APS} and BBT_{AEAPS}) as partial replacements of cement in concrete. The chemical modifications were realized with Brazilian bentonite sample, 3-aminopropyltrietoxisilane (APS) and 3,2-aminoethylaminopropyltrimetoxisilane (AEAPS), such as raw material and intercalating agents, respectively. These new functionalized compounds were characterized through physical and chemical methods. The results obtained with tests reveal the feasibility to develop to low cost concrete using natural and intercalated Amazon bentonite. The fabrication process will reduce megawatts of energy for production of concrete and greenhouse gases related to cement obtainment as well improve the longevity of the systems and the energetic influence of the organo-bentonite of adsorption/absorption of calcium nitrate was investigated.

2. Materials and Methods

2.1 Reagents and Raw Material

Bentonite sample employed in this investigation was extracted from a new deposit in the Amazon region, in northern Brazil. The natural bentonite sample, named BBT, with <2.0 μm particles, was separated by sedimentation. The CEC was measured in order to evaluate the potential use of clay for intercalation, following the ammonium acetate method with concentrations of 2.0 mol dm^{-3} at pH 8.0. The result obtained was 92.0 meq/100 g of clay on an air-dried basis. Chemical characterization was also carried out, using analytical techniques that will be described below. The natural silicate sample was activated in a stream of dry nitrogen by heating at 423 ± 1 K for ~10 h and used immediately.

Portland cement confirming to American Society for Testing and Materials (ASTM 2004) was utilized. The chemical and physical properties of cement are presented in Table 1, was named POR. For each blend, the experiment: normal consistency (%), workability (slump values %) of concrete and water adsorption (%) were determined in concordance with ASTM (C187-98, C109/C, C39/C, and C642-97) (Memon et al. 2012). The density of fresh concrete (Kg m^3) was determined by utilizing factor apparatus as mentioned by Memon et al. (2012) and described by Neville (2000).

Reagent grade solvents were used. The compounds *n*-dodecylamine [$CH_3(CH_2)_{11}NH_2$/≥ 99 %] (Sigma-Aldrich) and 3-aminopropyltrietoxisilane [$H_2N(CH_2)_3Si(OC_2H_5)_3$/ 99 %] (Sigma-Aldrich) and [3,(2-aminoethyl)aminopropyl]trimetoxisilane [$C_8H_{22}N_2O_3Si$/99 %] (Sigma-Aldrich) were used without purification. Other chemicals such as methanol and ethanol were of reagent grade. Stock standard solution 5,000.0 mg dm^{-3} of nitrate de calcium, was obtained from $Ca(NO_3)_2$ (Aldrich). The pH was adjusted by addition of 0.10 mol dm^{-3} of HNO_3 (Aldrich) or NaOH (Aldrich). Doubly distilled deionized water (DDW) was used for the preparation of solutions, wherever required. Solutions of $Ca(NO_3)_2$ were prepared from suitable serial dilution of the stock solution in DDW.

2.2 Chemical Modification of BBT

The organobentonite types were synthesized by maintaining the reagent molar ratios as 1:200:50:0.3, respectively, for *n*-dodecylamine, DDW, ethanol, and silylating agents. In the first step, *n*-dodecylamine was mixed with DDW and ethanol and allowed to stir continuously for 45 min. In the second step, ~5 g of BBT was added to the mixture and the stirring was continued for 50 min. During this time period the silylating agent 3-aminopropyltrietoxisilane was added drop-wise to form the final hybrid material. Same experimental procedure that was used for functionalization with APS, was utilized for functionalization with [3,(2-aminoethyl)aminopropyl]trimetoxisilane. After addition of silylating agents in the bentonite samples, the resulting mixture was further stirred for 20 h at 291 ± 1° K. At the end of the above process, the material was centrifuged, washed with DDW and air dried at room temperature for 30 h. The final products were named: BBT_{APS} and BBT_{AEAPS} and these materials were filtered, washed with toluene and ethanol, and dried under vacuum at 230 ± 1° K for ~15 h. The silylating agents were anchored in the reactive sites naturally and originality anchored on the surface BBT, such as hydroxyls groups, the density and disposition of reactive sites on the bentonite structure will govern the entrance and disposition of silylating organic molecule on the layer structure of phyllosilicate (Fig. 1).

2.3 Preparation of Cement-Bentonite Blends

Twenty-four blends samples were prepared with different proportions of natural and modified bentonite as partial replacements of cement in concrete. The blend were named: POR/BBT, POR/BBT_{APS}, and POR/BBT_{AEAPS} and the blends include 2, 5, 10, 15, 20, 25, 30, and 35 % by weight of cement. The blends samples were designed for compressive strength of 30 MPa.

2.4 Thermal Effect $Ca(NO_3)_2$ Interactions

The thermal effects from $Ca(NO_3)_2$ interacting on POR/BBT, POR/BBT_{APS}, and POR/BBT_{AEAPS} blends were followed by calorimetric titrations using an isothermal calorimeter, Model LKB 2277, from thermometric. In this titration, the $Ca(NO_3)_2$ solutions were added to a suspension of about 20 mg of the solid sample in 2.0 cm^3 of water,

Table 1 Surface area (SA_{BET}), real density (RD), porosity, CEC, and percentages of carbon (C), hydrogen (H), and nitrogen (N) for natural and modified bentonite clays and comparison of the properties natural and modified nontronite with some bentonite samples.

Sample	SA_{BET} ($m^2\ g^{-1}$)	RD ($g\ cm^{-3}$)	Porosity (%)	CEC[a] (mmol/100 g)	CEC[b] (mmol/100 g)	C (%)	H (%)	N (%)	C/N (calculated)	C/N (found)	References
BBT	34.2	0.992	29.325	98.8	109.4	0.016	0.093	–	–	–	Current research
BBT_{APS}	597.4	2.734	68.473	108.4	124.5	4.412	7.895	0.635	6.948	9	Current research
BBT_{AEAPS}	612.1	2.823	72.153	135.1	155.5	1.758	6.792	0.439	4.005	4	Current research
Imp-B	31.5	–	–	88.7	–	–	–	–		–	Sun et al. (2007)
PRYL-B	71.1	–	–	98.4	–	–	–	–	–	–	Sun et al. (2007)
Ca-bentonite	20	–	–	60.68	–	–	–	–	–	–	Ding et al. (2009)
Na-bentonite	56	–	–	94.30	–	–	–	–	–	–	Ding et al. (2009)

[a] 298 ± 1 K.
[b] 373 ± 1 K.

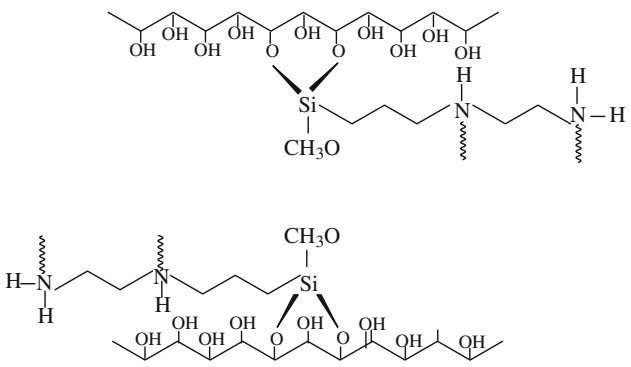

Fig. 1 Schematic representation of APS anchored in hydroxyl groups on the lamellar structure of phyllosilicate and disposition in the interlayer space.

under stirring at 298 ± 1° K. A series of increments of 10.0 dm^3 of $Ca(NO_3)_2$ solutions was added to the calcium nitrate molecules anchored in the cement + bentonite surface to obtain the thermal effect of interactions ($\sum Q_t$). Two other titrations are needed to complete the full experiment: (i) the thermal effect due to hydration of the blend samples ($\sum Q_h$), which normally gives a null value, and (ii) the dilution effect of $Ca(NO_3)_2$ solution in DDW, without sample in the vessel ($\sum Q_d$). The resulting thermal effect ($\sum Q_r$) is given by the following Eq. (1) (Guerra et al. 2011):

$$\sum Q_r = \sum Q_t - \sum Q_d - \sum Q_h \tag{1}$$

2.5 Characterization Methods

The elemental analysis (%C, %H, and %N) was determined on a Perkin Elmer 2400 Series II microelemental analyzer, and at least two independent determinations were performed for natural and modified bentonite samples.

The CEC of natural and modified bentonite clay samples were followed by the ammonium acetate method with a concentration of 2.0 mol dm^{-3} at pH 8.0 and six different temperatures (T_n = 298, 323, 348, 373, 393, and 413 ± 1° K).

The original and modified bentonite samples were analyzed by scanning electron microscopy (SEM) in JEOL microscope, model JEOL JSM 6360LV, using an acceleration voltage of 20 kV and magnification ranging from 200 to 500-fold. EDX analysis was carried out 80 kV; the bentonite spectrum was collected for 60 s.

The values of Brunauer–Emmett–Teller (BET) surface area, pore diameter and pore volume for each sample were obtained from nitrogen adsorption/desorption in a Micromeritics ASAP 2000 BET surface analyzer system. The mesopore size distribution was obtained by applying the Barret-Joyner-Halenda (BJH) method to the adsorption branch of the isotherm. The theoretical BET model for multilayer sorption is given by Eq. (2) (Weber 1972).

$$N_f = \frac{BQ^0 C_{Eq}}{(C_S - C_{Eq})\left[1 + (B-1)\left(\frac{C_{Eq}}{C_S}\right)\right]} \tag{2}$$

where C_S is the saturation concentration, B is the constant indicating the energy of solute-surface interaction, C_{Eq} is the equilibrium concentration, and Q^0 is the constant indicating the amount of solute adsorbent forming a complete monolayer.

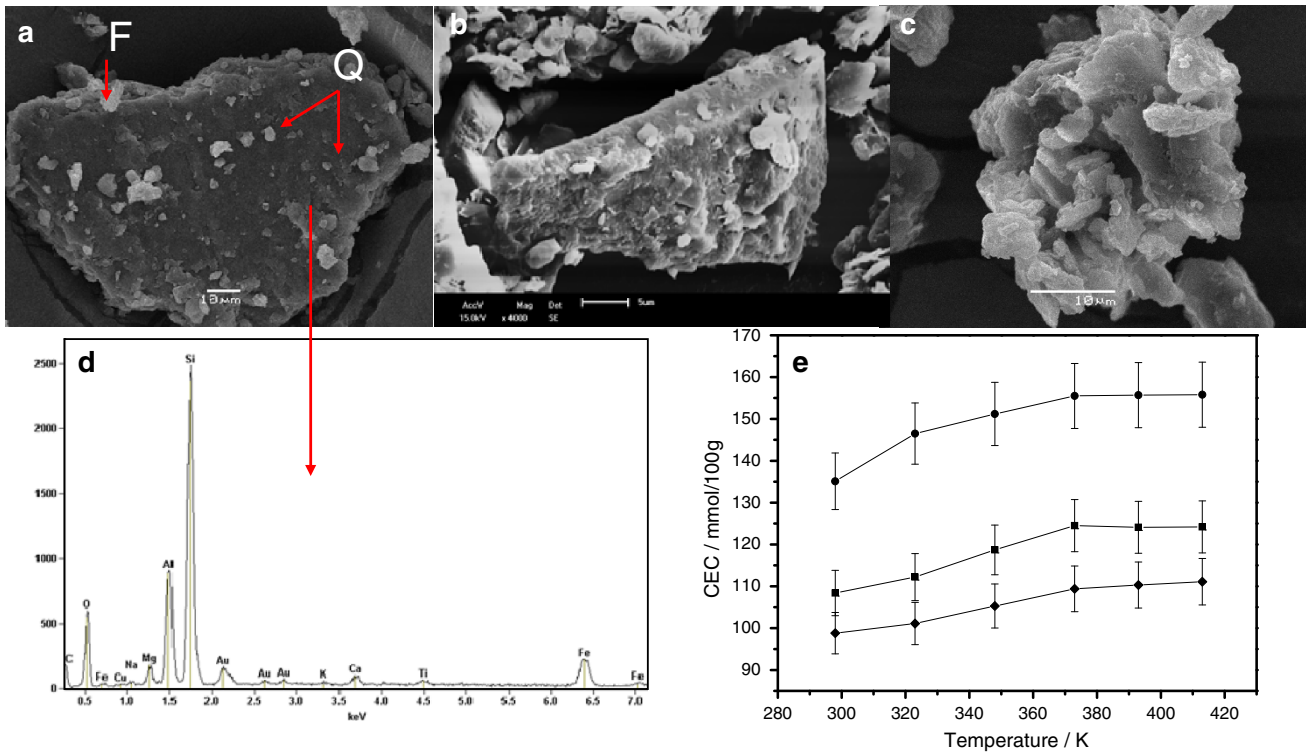

Fig. 2 SEM micrographs of the natural and modified bentonite samples: BBT (**a**), BBT_{APS} (**b**), BBT_{AEAPS} (**c**), chemical analysis (EDX) of raw bentonite, BBT (**d**) and evolution of CEC in different temperatures, BBT *filled diamond*, BBT_{APS} *filled square*, and BBT_{AEAPS} *filled circle* (**e**).

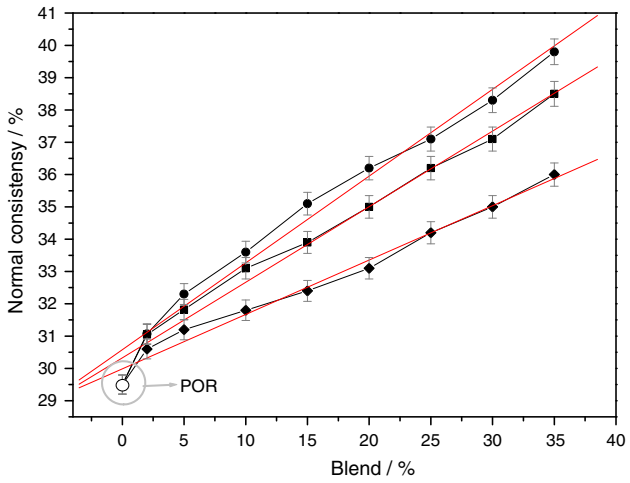

Fig. 3 Consistency for POR *open diamond*, POR/BBT *filled diamond*, POR/BBT_{APS} *filled square*, and POR/BBT_{AEAPS} *filled circle* in different mixes.

3. Results and Discussion

3.1 Characterization of Bentonite and Organobentonite

The preliminary characterizations of natural bentonite sample reveal that the mineral component principal in this clay sample is the interstratified smectite–illite (S–I) and secondary minerals were identified as feldspar and quartz. In these formed 2:1 silicate structures the organic part is distributed inside the interlayer lamellar cavity of interstratified S–I and the percentages of carbon, hydrogen, and nitrogen content are listed in Table 1, with the integrity of the organic molecules being present in the dioctahedral 2:1 structure of S–I confirmed from the calculated C/N ratios (Ruiz and Airoldi 2004). Based on the analytical data for BBT and two organic–inorganic materials, the density of these pendant organic molecules immobilized on the tetrahedral silica layer of the phyllosilicate can be calculated. Thus, the precursor $H_2N–(CH_2)_3Si(OC_2H_5)_3$ agent grafted onto bentonite clay gave an amount of 6.942 mmol g^{-1} (BBT_{APS}). In principle, this small pendant molecule density should be expected as a consequence of its large volume, which could cause a degree of hindrance to impede the reaction.

Typical SEM micrographs of powder original and modified bentonite were presented in Fig. 2a to 2c, respectively. The micrographs reveal the heterogeneous nature of surface morphology of the clay sample which also shows that S–I crystals to possess a foliated crystal like morphology. In the BBT micrograph was also observed crystals of small size belonging to the hexagonal crystalline system, these crystals can be attributed the accessory mineral quartz (Fig. 2a), this is relatively common in the Amazon soil and in other regions in South America, and the formation of mineral is propitiated by lixiviation of Amazon soil, where the intemperism powered by the Amazon clime may produce clay minerals as kaolinite, illite, etc. from feldspar mineral. The crystals present some fissures, this fissures were best visualized in the SEM of modified bentonite samples (Fig. 2b and 2c), which can be indicating the presence of a macroporous structure. These, should contribute significantly to the diffusion of the organic chain to the silicate adsorbent surfaces, favoring de organofunctionalization process with long

organic chain and posteriorly the incorporation of $Ca(NO_3)_2$. In Fig. 2d is presented chemical analyses for BBT samples (EDX), the presence of silicon, aluminum, magnesium, and iron was observed and can be attributed to principal component (S–I) and accessory minerals (Q and F), the small perceptual of carbon was presented; the carbon presence can be attributed to remnants of organic material from humic substances, naturally adhered to bentonite sample by the direct influence of abundant and peculiar Amazon biota (Xifang et al. 2007). The EDX of BBT showed high iron content; this occurrence can be attributed to presence of hematite mineral (Fe_2O_3) in BBT sample. This mineral is rich in Fe(II) and Fe(III) and common in weathered soils, such as Amazon soil. These soils are formed under moist climates and elevated temperature (308–318 K), i.e., characteristics of tropical climates.

The textural analyses have been important for investigation of the reactive centers in the surface of functionalized

Table 2 Blend design.

Component	0 %[a]	2 %	5 %	10 %	15 %	20 %	25 %	30 %	35 %
POR/BBT									
Cement (kg m^{-3})	360.0	352.8	342.0	324.0	306.0	288.0	270.0	252.0	234.0
Bentonite (kg m^{-3})	0.0	7.2	18.0	36.0	54.0	72.0	90.0	108.0	126.0
Fine aggregate (kg m^{-3})	830.0	830.0	830.0	830.0	830.0	830.0	830.0	830.0	830.0
Coarse aggregate (kg m^{-3})	1,015.0	1,015.0	1,015.0	1,015.0	1,015.0	1,015.0	1,015.0	1,015.0	1,015.0
Water (kg m^{-3})	201.0	201.0	201.0	201.0	201.0	201.0	201.0	201.0	201.0
POR/BBT_{APS}									
Cement (kg m^{-3})	370.0	362.6	351.5	333.0	314.5	296.0	277.5	259.0	240.5
Bentonite (kg m^{-3})	0.0	7.4	18.5	37.0	55.5	74.0	92.5	111.0	129.5
Fine aggregate (kg m^{-3})	835.0	835.0	835.0	835.0	835.0	835.0	835.0	835.0	835.0
Coarse aggregate (kg m^{-3})	1,021.0	1,021.0	1,021.0	1,021.0	1,021.0	1,021.0	1,021.0	1,021.0	1,021.0
Water (kg m^{-3})	205.0	205.0	205.0	205.0	205.0	205.0	205.0	205.0	205.0
POR/BBT_{AEAPS}									
Cement (kg m^{-3})	380.0	372.4	361.0	342.0	323.0	304.0	285.0	266.0	247.0
Bentonite (kg m^{-3})	0.0	7.6	19.0	38.0	57.0	76.0	95.0	114.0	133.0
Fine aggregate (kg m^{-3})	841.0	841.0	841.0	841.0	841.0	841.0	841.0	841.0	841.0
Coarse aggregate (kg m^{-3})	1,019.0	1,019.0	1,019.0	1,019.0	1,019.0	1,019.0	1,019.0	1,019.0	1,019.0
Water (kg m^{-3})	208.0	208.0	208.0	208.0	208.0	208.0	208.0	208.0	208.0

[a] Ordinary Portland cement (OPC) pure.

materials and are an indicative of the potential of the materials in study, for application in adsorption process. The surface area of a porous organoclay is one of the most useful microstructural parameters for defining properties. The BET surface area values of the natural and modified bentonite samples demonstrated that chemical modification caused the formation of micropores in the solid particles, resulting in a higher surface area, revealing 612.1 $m^2\ g^{-1}$ for BBT_{AEAPS} and relative to the natural BBT sample with 34.1 $m^2\ g^{-1}$. The values of micropore area change in the same direction, varying from 7.2 $m^2\ g^{-1}$ for the BBT to 12.3 $m^2\ g^{-1}$ for the BBT_{AEAPS}. The textural properties of natural and modified bentonite samples are reported in Table 1, which depends on particle size shape, and distribution of cracks and pores in the material, the surface area and CEC of bentonite samples used and obtained in these studies were compared with other bentonite samples studied by Sun et al. (2007) and Ding et al. (2009). The BBT_{AEAPS} has a significantly higher surface area than the BBT and has pores <2 nm in diameter (micropore) in addition to some mesopores (>4 nm in diameter). The natural bentonite has small N_2 BET surface areas and only mesopores because N_2, as opposed to H_2O, OH^-, and H_3O^+, is unable to penetrate into the octahedral position in structure of interstratified S–I may have in the centre a vacancy.

The CEC of clay mineral is attributed to structural defects, broken bonds and structural hydroxyl transfers (Jänchen et al. 2009). Intercalation process increases the total number o exchange sites marginally in bentonite. The CEC is relatively high compared to outer occurrence of bentonite clay, for comparison. The CEC of natural bentonite was found to be 98.8 mmol/100 g of clay, and BEN_{AEAPS} was found to be 135.1 mmol/100 g of clay, as listed in Table 1. The CEC of bentonite types were studied in six temperatures. The CEC values increased in the high temperature, the CEC values was increased in 10.74, 14.81, and 15.12 % for BBT_{APS}, BBT_{AEAPS}, and BBT, respectively, in 4 h, at 373 ± 1 K (Fig. 2e). The structural expansion of minerals that are components of BBT samples can be attributed to increase of temperature and organofunctionalization process. This explanation is based in the accessibility of the sites rich in reactive ions, like as OH^-, and H_3O^+. This accessibility was caused by entrance of organic molecule in the mineral structure and thermal expansion of layers of silicates.

3.2 Consistency, Workability, and Density of Concrete

The consistency, workability, and density of concrete were important properties that reveal factors such as the durability and kinetic mechanism of drying of concrete. The normal consistency results obtained with cement pastes containing different perceptual of BBT, BBT_{APS}, and BBT_{AEAPS} were presented in Fig. 3. The comparison of perceptual is clearly observed that water requirement to make the paste of standard consistency increased with the increase in bentonite content, principally in functionalized form. The BBT_{APS} and BBT_{AEAPS} presented substantial specific area (Table 1) and the particle size and functionalization process of bentonite

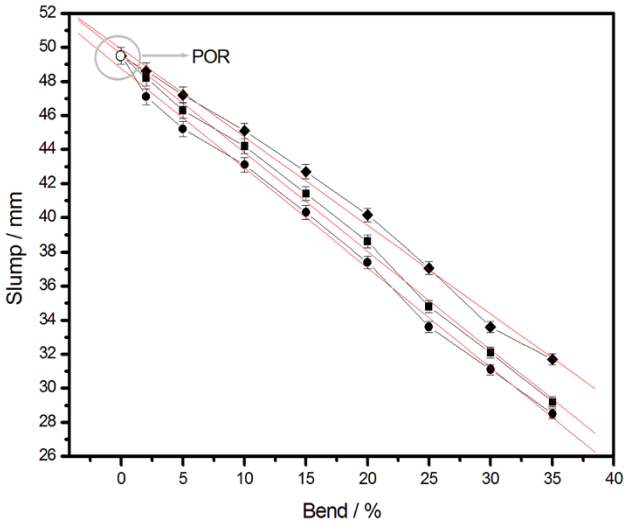

Fig. 4 Slump values for POR *open circle*, POR/BBT *filled diamond*, POR/BBT_{APS} *filled square*, and POR/BBT_{AEAPS} *filled circle* in different mixes.

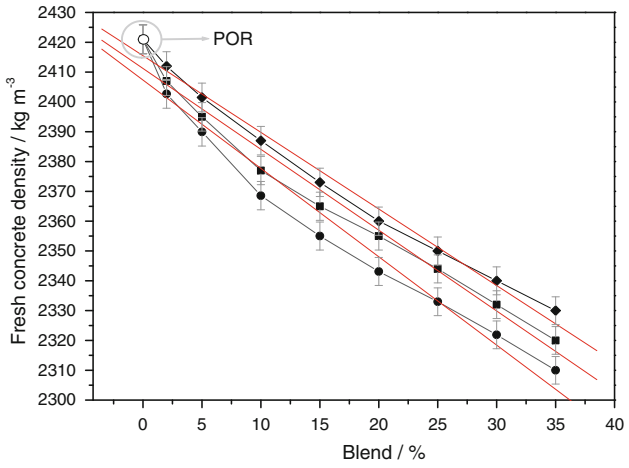

Fig. 5 Fresh concrete density for POR *open circle*, POR/BBT *filled diamond*, POR/BBT_{APS} *filled square*, and POR/BBT_{AEAPS} *filled circle* in different mixes.

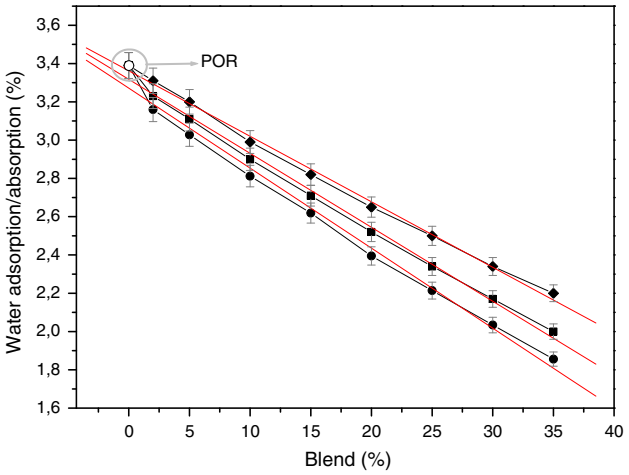

Fig. 6 Water adsorption/absorption for POR *open circle*, POR/BBT *filled diamond*, POR/BBT_{APS} *filled square*, and POR/BBT_{AEAPS} *filled circle* in different mixes.

Table 3 Mathematical models for each experiment obtained by experiment results with linear regression.

Experiment	Representative equation	R^2
POR/BBT		
Normal consistency (%)	$Y(x) = 29.98864 \pm 0.15717 + 0.16833 \pm 0.00797x$	0.99225
Workability-slump (mm)	$Y(x) = 49.90874 \pm 0.27287 - 0.51795 \pm 0.01831x$	0.99754
Fresh concrete density (kg m^{-3})	$Y(x) = 2415.47177 \pm 2.08158 - 2.56863 \pm 0.10551x$	0.99415
Water adsorption/absorption (%)	$Y(x) = 3.36211 \pm 0.01476 - 0.03422 \pm 7.47965E-4x$	0.99833
POR/BBT$_{APS}$		
Normal consistency (%)	$Y(x) = 30.32881 \pm 0.22071 + 0.23388 \pm 0.01119x$	0.99209
Workability-slump (mm)	$Y(x) = 49.59246 \pm 0.21938 - 0.57769 \pm 0.01112x$	0.99871
Fresh concrete density (kg m^{-3})	$Y(x) = 2411.21326 \pm 3.02437 - 2.71069 \pm 0.15328x$	0.98899
Water adsorption/absorption (%)	$Y(x) = 3.31769 \pm 0.02035 - 0.03866 \pm 0.000103x$	0.99752
POR/BBT$_{AEAPS}$		
Normal consistency (%)	$Y(x) = 30.58139 \pm 0.32074 + 0.26857 \pm 0.01626x$	0.98742
Workability-slump (mm)	$Y(x) = 48.76775 \pm 0.28041 - 0.58528 \pm 0.01421x$	0.99794
Fresh concrete density (kg m^{-3})	$Y(x) = 2407.31531 \pm 4.28739 - 2.96196 \pm 0.21729x$	0.98168
Water adsorption/absorption (%)	$Y(x) = 3.27142 \pm 0.03162 - 0.04179 \pm 0.000161x$	0.99489

samples increased the porous volume of the whole mix translating into higher water molecules to wet the surface area organic–inorganic and interior of pores. The process can be classified as diffusional process, i.e., in the bentonite structure samples can be occurred adsorption and absorption processes, simultaneously. The mixes were designed for compressive strength of 30 MPa. The details are summarized in Table 2.

The workability results obtained with cement pastes containing amount of BBT, BBT$_{APS}$, and BBT$_{AEAPS}$ were presented in Fig. 4. The slump values, this empirical test that measures the workability of fresh concrete. The results reveal that workability decreased as the amount of natural bentonite, same behavior is observed for bentonite functionalized, principality for POR/BBT$_{AEAPS}$. The diminution of slump values is due to the small particle size, particles that were components of bentonite samples, and optimization of the textural properties of natural bentonite with functionalization process. It can therefore be indicated that for the same water binder ratio, concrete made BBT, BBT$_{APS}$, and BBT$_{AEAPS}$ is less workable than the POR.

The results of fresh density of new concrete obtained with cement pastes containing amount of BBT, BBT$_{APS}$, and BBTA$_{EAPS}$ were presented in Fig. 5. The tests reveal that density of POR in fresh state is presented as maximum value obtained with all experiments, 2,422.0 kg m^{-3}. The density values decreased with the addition of amount of bentonite samples as cement replacement, and higher the bentonite perceptual lower is the density. This is due to the fact that the density being a function of specific gravity. In the other studies, the specific gravity of Portland cement is more as compared to Pakistani bentonite sample (Memon et al. 2012). These studies shown similar conclusion, the density of the samples of cement with bentonite was highest for all experiments.

3.3 Water Adsorption/Absorption

The water adsorption and absorption results obtained with cement pastes containing amount of BBT, BBT$_{APS}$, and BBT$_{AEAPS}$ were presented in Fig. 6. Experiments data shown that water adsorption/absorption process decreased as the cement substitution by natural bentonite amount increased. The decrease can be attributed to the fact that chemical reaction between natural pozzolans and hydroxyl molecules of hydrated POR paste is lime consuming instead of lime producing; the particle size of natural bentonite sample is less than that of cement therefore it can pack the binder phase and hence reduce porosity. In the tests with functionalized bentonite the adsorption/absorption of water decreased as the POR substitution by functionalized bentonite increased. The behaviour can be explained to the fact that reaction of organic molecules inserted in bentonite structure by functionalization process, this molecules are not chelating agents for water molecules. In the calorimetric studies, the hydration effect generally is considered null. The experimental results were modeled mathematically, the representative equations for normal consistency, workability, fresh concrete density, and water adsorption/desorption were presented in Table 3.

3.4 Thermodynamic Effects of Presence of $Ca(NO_3)_2$

The effects of $Ca(NO_3)_2$ based corrosion inhibitor and crack width on the corrosion process of steel reinforcing bars in high performance concrete are important for manufacturing of

Table 4 Thermodynamic data for $Ca(NO_3)_2$ interaction (adsorption/absorption) onto OPC and bentonite blends (material 1.0 g dm^{-3}, time 400 min, and temperature 298 ± 1° K).

Thermodynamic data	0 %[a]	2 %	5 %	10 %	15 %	20 %	25 %	30 %	35 %
POR/BBT									
$\Delta_{int}h$ (J g^{-1})	21.5 ± 0.2	35.2 ± 0.1	44.0 ± 0.1	51.6 ± 0.1	78.4 ± 0.2	117.3 ± 0.1	129.0 ± 0.1	130.0 ± 0.3	131.2 ± 0.1
$\Delta_{int}H$ (kJ mol^{-1})	4.3 ± 0.1	4.4 ± 0.3	4.4 ± 0.3	4.5 ± 0.1	4.9 ± 0.1	6.9 ± 0.2	7.5 ± 0.2	7.3 ± 0.2	7.2 ± 0.2
$\Delta_{int}G$ (kJ mol^{-1})	18.0 ± 0.1	18.0 ± 0.1	18.1 ± 0.1	18.3 ± 0.4	19.0 ± 0.2	20.9 ± 0.2	21.8 ± 0.2	21.6 ± 0.3	21.5 ± 0.1
$\Delta_{int}S$ (JK^{-1} mol^{-1})	46 ± 1	46 ± 1	46 ± 1	46 ± 1	47 ± 1	47 ± 1	48 ± 1	48 ± 1	48 ± 1
R^2	0.99999	0.99999	0.99999	0.99999	0.99998	0.99999	0.99999	0.99999	0.99999
POR/BBT_{APS}									
$\Delta_{int}h$ (J g^{-1})	21.5 ± 0.2	41.3 ± 0.3	56.4 ± 0.1	65.4 ± 0.4	82.5 ± 0.1	171.8 ± 0.5	180.7 ± 0.1	181.5 ± 0.1	182.1 ± 0.4
$\Delta_{int}H$ (kJ mol^{-1})	4.3 ± 0.1	5.8 ± 0.1	6.5 ± 0.3	6.7 ± 0.1	7.3 ± 0.1	7.4 ± 0.1	7.7 ± 0.1	7.7 ± 0.2	7.7 ± 0.1
$\Delta_{int}G$ (kJ mol^{-1})	18.0 ± 0.1	19.8 ± 0.1	20.5 ± 0.2	20.7 ± 0.1	21.6 ± 0.3	21.7 ± 0.1	22.3 ± 0.1	22.3 ± 0.1	22.3 ± 0.3
$\Delta_{int}S$ (JK^{-1} mol^{-1})	46 ± 1	47 ± 2	47 ± 2	47 ± 2	48 ± 2	48 ± 2	49 ± 2	49 ± 2	49 ± 2
R^2	0.99999	0.99999	0.99999	0.99999	0.99998	0.99999	0.99999	0.99999	0.99997
POR/BBT_{AEAPS}									
$\Delta_{int}h$ (J g^{-1})	21.5 ± 0.2	45.6 ± 0.1	61.2 ± 0.1	68.5 ± 0.1	87.1 ± 0.1	185.6 ± 0.1	187 ± 0.1	189.7 ± 0.1	190.8 ± 0.1
$\Delta_{int}H$ (kJ mol^{-1})	4.3 ± 0.1	6.8 ± 0.3	6.8 ± 0.1	6.8 ± 0.1	7.5 ± 0.1	7.5 ± 0.1	7.9 ± 0.1	7.9 ± 0.1	7.9 ± 0.2
$\Delta_{int}G$ (kJ mol^{-1})	18.0 ± 0.1	21.1 ± 0.2	21.1 ± 0.1	21.1 ± 0.2	22.1 ± 0.1	22.1 ± 0.3	22.8 ± 0.1	22.8 ± 0.2	22.8 ± 0.1
$\Delta_{int}S$ (JK^{-1} mol^{-1})	46 ± 1	48 ± 2	48 ± 2	48 ± 2	49 ± 2	49 ± 2	50 ± 2	50 ± 2	50 ± 2
R^2	0.99999	0.99998	0.99999	0.99997	0.99999	0.99999	0.99999	0.99998	0.99998

[a] Ordinary Portland cement (OPC) pure.

structure with high resistance and durability, the thermodynamic effects of adhesion of calcium nitrate in concrete may contribute for understanding mechanisms of corrosion inhibition. The thermodynamic effects of $Ca(NO_3)_2$ presence in POR, POR/BBT, POR/BBT_{APS}, and POR/BBT_{AEAPS} was studied by a series of calorimetric titrations, the number of increments and the volumes of $Ca(NO_3)_2$ solution needed to saturate the mass of the cement + bentonite blend types were listed in Table 4.

The isotherm data obtained from the calorimetric titrations were used in a $\Sigma\Delta_r h$ versus ΣX plot and the non-linearized form is given by a $\Sigma X/\Sigma\Delta_r h$ versus ΣX plot are presented in Fig. 7a (Ruiz and Airoldi 2004). From the enthalpy of formation of monolayer $\Delta_{int}h$ and the number of moles of water, N_s, adsorbed, on the materials, the enthalpies of interaction can be calculated by Eq. (3).

$$\Delta_{int}H = \frac{\Delta_{int}h}{N_S} \tag{3}$$

Change in free energy ($\Delta_{int}G$), enthalpy ($\Delta_{int}H$), and entropy ($\Delta_{int}S$) are important thermodynamic parameters that were determined using the following equations (Eqs. (4) and (5)), taking these values into account (Malkoc and Nuhoglu 2005):

$$\Delta_{int}G = -RT\ln K_L \tag{4}$$

where K_L is the equilibrium constant obtained from the Langmuir isotherm equation, T is the absolute temperature, and R is the universal gas constant (8.314×10^{-3} kJ K^{-1} mol^{-1}). Equation (5) relates the energetic of bend systems (Malkoc and Nuhoglu 2005).

$$\Delta_{int}G = \Delta_{int}H - T\Delta_{int}S \tag{5}$$

The thermodynamic cycle for this series of adhesion of calcium processes involving suspension (susp) of POR, POR/BBT, POR/BBT_{APS}, and POR/BBT_{AEAPS} (POR/BBT_x) in aqueous solution (aq) with $Ca(NO_3)_2$ solutions (CN), can be represented by the following calorimetric reactions. Reactions 6–8 represent calorimetric titration experiment carried out in duplicate for each calorimetric determination (Ruiz and Airoldi 2004; Guerra et al. 2012):

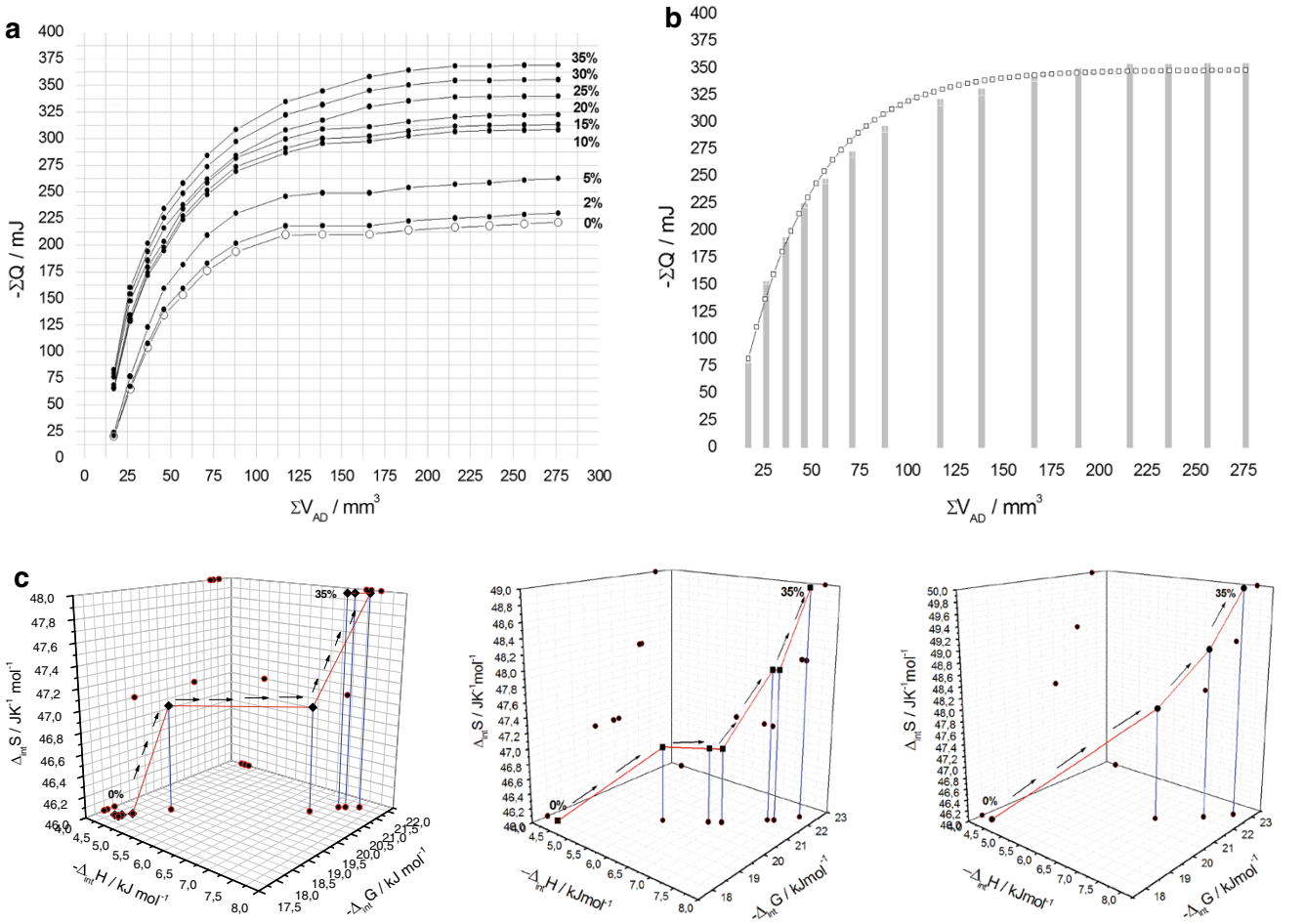

Fig. 7 Isotherms of thermal effects for $Ca(NO_3)_2$ interaction for POR *open circle* and POR/BBT_{AEAPS} *filled circle* (**a**), an example of isotherm calculated with non-linear method [POR/BBT_{AEAPS}/$Ca(NO_3)_2$] (**b**), and relationship between thermodynamics interaction values for three systems, POR/BBT *filled diamond*, POR/BBT_{APS} *filled square*, and POR/BBT_{AEAPS} *filled circle* (**c**).

$$\mathrm{POR/BBT}_{x(\mathrm{susp})} + \mathrm{CN}_{(\mathrm{aq})} \rightarrow \mathrm{POR/BBT}_x \times \mathrm{CN}_{(\mathrm{susp})} \quad \Sigma Q_t \tag{6}$$

$$\mathrm{POR/BBT}_{x(\mathrm{susp})} + \mathrm{nH_2O} \rightarrow \mathrm{BBT}_x \times \mathrm{nH_2O}_{(\mathrm{aq})} \quad \Sigma Q_h \tag{7}$$

$$\mathrm{CN}_{(\mathrm{aq})} + \mathrm{nH_2O} \rightarrow \mathrm{CN} \times \mathrm{nH_2O}_{(\mathrm{aq})} \quad \Sigma Q_d \tag{8}$$

The thermal effects of reactions 6–9 for each experimental point of the calorimetric titration obtained with insertions of calcium solutions on blend portions were considered in the calculation of the net thermal effect (ΣQ_r) of these interactions, as represented by reaction 9.

$$\mathrm{POR/BBT}_x \times \mathrm{nH_2O}_{(\mathrm{aq})} + \mathrm{CN} \times \mathrm{nH_2O}_{(\mathrm{aq})} \rightarrow \mathrm{POR/BBT}_x \times \mathrm{CN}_{(\mathrm{susp})} \quad \Sigma Q_r \tag{9}$$

The thermodynamic data were summarized and listed in Table 4. From the thermodynamic point of view, the obtained exothermic and positive entropic values establish the set of favourable results for the thermodynamic of CN-POR/BBT$_x$ interactions. Thus, the spontaneities of such reactions are expressed by the negative Gibbs free energy with a considerable contribution of the positive entropy. These values suggest that, during interactions $Ca(NO_3)_2$ molecules and reactive sites on the blend surfaces, the desolvation disturbs the structure of the reaction medium to promote the disorganization of the system and, consequently, leads to an increase in entropy (Ruiz and Airoldi 2004; Guerra et al. 2012). An example of isotherm calculated with non-linear method for system POR/BBT$_{AEAPS}$/CN was shown in Fig. 7b and relationship between thermodynamics adsorption values for three systems was presented in Fig. 7c. This relationship reveals the effect of complexity of structure of blends in the energetic reaction involving $Ca(NO_3)_2$ incorporation processes. In conclusion, all thermodynamic values are favourable, with exothermic enthalpy, negative free Gibbs energy and positive entropy, data corroborate with CN-POR/BBT$_x$ interactions at the solid (blends)/liquid interface ($Ca(NO_3)_2$ solution).

4. Concluding Remarks

The low cost concrete can be produced by introduction of clay minerals such as bentonite as partial replacements of cement in concrete without compromising on strength parameters and durability of concrete. The following points are draw from study carried out to date:

(i) The physicochemical properties of BBT were optimized by functionalization process. The density of these pendant organic molecules immobilized on the tetrahedral silica layer of the phyllosilicate can be calculated. Thus, the precursor APS agent grafted onto bentonite clay gave an amount of 6.942 mmol g^{-1} for BBT$_{APS}$. The CEC values increased in the high temperature, the CEC values was increased in 10.74, 14.81, and 15.12 % for BBT$_{APS}$, BBT$_{AEAPS}$, and BBT, respectively. The values of micropore area change in the same direction, varying from 7.2 m^2 g^{-1} for the BBT to 12.3 m^2 g^{-1} for the BBT$_{AEAPS}$. In conclusion, two new chelating materials were synthesized with success by organo-functionalization methods, these methods can be used with other intercalating agents and new phyllosilicate occurrences.

(ii) The utilization of organofunctionalized bentonite as pozzolan is a good option of the point of view environmental, financial and technical, the bentonite is a clay mineral highly abundant in various parts of the world. The consistence, workability, density of concrete, and water adsorption/absorption were decreased with the insertion of natural and functionalized bentonite as partial cement replacements in all experiments. The results reveal that workability decreased with decrease of the amount of natural bentonite in the concrete, same behavior is observed for bentonite functionalized, varying from 49 mm (POR) to 28 mm (POR/BBT$_{AEAPS}$).

(iii) The results of $Ca(NO_3)_2$ adsorption/absorption were confirmed through stable complexes formed between cations and reactive groups disposed on the surface blends, whose behavior was checked by the thermodynamic values obtained by calorimetric investigations at the solid/liquid interface to give favourable sets of data, thermodynamic values calculation showed that the $Ca(NO_3)_2$ molecules adsorption process by blends has exothermic and naturally spontaneous, such as exothermic enthalpy (21.5 to 131.2 J g^{-1}), negative Gibbs free energy (18.0 to 21.5 kJ mol^{-1}), and positive entropic (46–48 JK^{-1} mol^{-1}) values. The incorporation process of $Ca(NO_3)_2$ molecules on blend samples were controlled by chemical and physical mechanisms.

(iv) Actuality a wide variety of pozzolan materials is utilized for the cement optimization; the ideal pozzolan mandatorily should be interesting characteristics for industrial and environmental applications, in this context, is possible conclude that the clay and organoclays employed are quite economic than commercially available pozzolans. Effect of concentration variation and introduction of corrosion inhibitor in the paste of cement will be important parameters affecting the concrete performance in the real application in construction industry in a near future, the advance and limitations of applications will be investigated in work futures.

Acknowledgments

The authors are grateful to MCT, CNPq, and CAPES for financial supports and fellowships.

Open Access

References

Ahmad, S., Barbhuiya, S. A., Elahi, A., & Iqbal, J. (2011). Effect of Pakistani bentonite on properties of mortar and concrete. *Clay Minerals, 46*, 85–92.

ASTM. (2004). Standard test method for normal consistency of hydraulic cement. C187-98C, In: S. J. Bailey, N. C. Baldini, E. K. McElrone, K. A. Peters (Eds.), Annual book of ASTM standards cement, Lime, Gypsum, 2004; (Vol. 4, pp. 180–181).

Bojumueller, A., Nennemann, G., & Lagaly, G. (2001). Enhanced pesticide adsorption by thermally modified bentonites. *Applied Clay Science, 18*, 277–284.

Bulut, G., Chimeddorj, M., Esenli, F., & Çelik, M. S. (2009). Production of desiccants from Turkish bentonite. *Applied Clay Science, 40*, 141–147.

Chaudhari, A., & Kumar, C. V. (2005). Intercalation of proteins into & #x03B1;-zirconium phosphates: tuning the binding affinities with phosphate functions. *Microporous and Mesoporous Materials, 77*, 175–187.

Dey, R., & Airoldi, C. (2008). Designed pendant chain covalently bonded to silica gel for cation removal. *The Journal of Hazardous Materials, 156*, 95–101.

Diaz, U., Cantin, A., & Corma, A. (2007). Novel layered organic–inorganic hybrid materials with bridged silsesquioxanes as pillars. *Chemistry of Materials, 19*, 3686–3693.

Ding, S., Sun, Y., Yang, C., & Xu, B. (2009). Removal of copper from aqueous solutions by bentonite and the factors affecting it. *Ministry of Science and Technology, 19*, 0489–0492.

Garvin, S. L., & Hayles, C. S. (1999). The chemical compatibility of cement-bentonite cut-off wall material. *Construction and Building Materials, 13*, 329–341.

Goubitz, K., Capková, P., Melánová, K., Molleman, W., & Schenk, H. (2001). Structure determination of two intercalated compounds $VOPO_4{\cdot}(CH_2)_4O$ and $VOPO_4{\cdot}OH–(CH_2)_2–O–(CH_2)_2–OH$; synchrotron power diffraction and molecular modeling. *Acta Crystallographica B, 57*, 178–183.

Guerra, D. L., Lemos, V. P., Airoldi, C., & Angélica, R. S. (2006). Influence of the acid activation of pillared smectites from Amazon (Brazil) in adsorption process with butylamine. *Polyhedron, 25*, 2880–2890.

Guerra, D. L., Mendonça, E. S., Silva, R. A. R., & Lara, W. (2012). Studies of adsorption of pillarized and organofunctionalized smectite clay for Th^{4+} removal. *The Journal of Ceramic Science and Technology, 3*, 17–28.

Guerra, D. L., Silva, E. M., Lara, W., & Batista, A. C. (2011a). Removal of Hg(II) from an aqueous medium by adsorption onto natural and alkil-amine modified Brazilian bentonite. *Clays and Clay Minerals, 59*, 568–580.

Guerra, D. L., Viana, R. R., & Airoldi, C. (2009). Adsorption of mercury cation on chemical modified clay. *Materials Research Bulletin, 44*, 485–491.

Guerra, D. L., Viana, R. R., & Airoldi, A. (2011b). Thermochemical data for *n*-alkylmonoamine functionalization into lamellar silicate al-kanemite. *The Journal of Chemical Thermodynamics, 43*, 69–74.

Jänchen, J., Morris, R. V., Bish, D. L., Janssen, M., & Hellwig, U. (2009). The H_2O and CO_2 adsorption properties of phyllosilicates poor palagonitic dust and bentonite under martin environmental conditions. *Icarus, 200*, 463–467.

Lazarin, A. M., & Airoldi, C. (2009). Thermodynamic of the nickel and cobalt removal from aqueous solution by layered crystalline organofunctionalized barium phosphate. *The Journal of Chemical Thermodynamics, 41*, 21–25.

Malkoc, E., & Nuhoglu, Y. (2005). Investigation of nickel(II) removal from aqueous solutions using tea factory waste. *The Journal of Hazardous Materials B, 127*, 120–128.

Memon, S. A., Arsalan, R., Khan, S., & Lo, T. Y. (2012). Utilization of Pakistan bentonite as partial replacement of cement in concrete. *Constructing Building Materials, 30*, 237–242.

Meunier, A. (2005). *Clays*. Berlin, Germany: Springer. 472.

Mirza, J., Riaz, M., Naseer, A., Rehman, F., Khan, A. N., & Ali, Q. (2009). Pakistan bentonite in mortars and concrete as low cost construction material. *Applied Clay Science, 45*, 220–226.

Neville, A. M. (2000). *Properties of concrete* (4th ed.). London, UK: Person Education Asia Pte. Ltd.

Ogawa, M., Ishii, T., Miyamoto, N., & Kuroda, K. (2003). Intercalation of a cationic azobenzene into montmorillonite. *Applied Clay Science, 22*, 179–185.

Plee, D., Lebedenko, F., Obrecht, F., Letellier, M., & Van Damme, H. (1990). Microstrucuture, permeability and reology of bentonite-cement slurries. *Cement Concrete Research, 20*, 45–61.

Ruiz, V. S. O., & Airoldi, C. (2004). Thermochemical data for *n*-alkylmonoamine intercalation into crytalline lamellar zirconium phenylphosphonate. *Thermochimica Acta, 420*, 73–78.

Shannag, M. (2000). High strength concrete containing natural pozzolan and silica fume. *Cement and Concrete Composites, 22*, 399–406.

Sharma, P., Singh, G., & Tomar, R. (2009). Synthesis and characterization of an analogue of heulandite: Sorption and applications for thorium(IV), europium(III), samarium(II) and iron(II) recovery from aqueous waster. *Journal of Colloid and Interface Science, 332*, 298–308.

Sun, X., Li, C., Wu, Z., Ren, L., & Zhao, H. (2007). Adsorption of protein from model wine solution by different bentonites. *Chinese Journal of Chemical Engineering, 15*, 632–638.

Taylor-Lange, S. C., Riding, K. A., & Juenger, M. C. G. (2012). Increasing the reactivity of metal kaolin-cement blends

using zinc oxide. *Cement and Concrete Composites, 34*, 834–847.

Weber, W. J. Jr. (1972). Adsorption. In W. J. Weber (Ed.), *Physicochemical process for water quality control*. New York, NY: Wiley.

Zhang, P., Wang, Y., Zhu, G. S., Shi, Z., Liu, Y. L., Yuan, H. M., et al. (2000). Hydrothermal synthesis and crystal structure of $Zn_4(PO_4)_2(HPO_4)2.0.5(C_{10}H_{28}N_4).2H_2O$ a new layered zinc phosphate with 12-ring cavities. *Journal of Solid State Chemistry, 154*, 368–374.